Derivation of aerosol optical properties using ground-based radiation measurements

T. Donth[1], E. Jäkel[1], B. Mey[2], M. Wendisch[1]

[1]*Institute for Meteorology, Stephanstr. 3, 04103 Leipzig*
[2]*Fraunhofer Institute for Wind Energy and Energy System Technology, Königstor 59, 34119 Kassel*

Abstract

The knowledge of the optical and microphysical properties of aerosol particles in the atmosphere is relevant in various scientific fields from public health issues to climate modeling. A retrieval method is presented that estimates the single scattering albedo and asymmetry parameter of aerosol particles in regions of high pollution using spectral ground-based radiance and irradiance measurements, radiative transfer simulations, and a priori knowledge of the aerosol optical depth (AOD) derived from sun photometer observations. The used measurement data originated from the Pearl River Delta in China. The results are compared with sun photometer data and show a high agreement for AODs larger than 0.5. For low AODs and for cloudy conditions the method did not work due to the strong sensitivity of the initial parameters.

Zusammenfassung

Kenntnisse über optische und mikrophysikalische Eigenschaften von Aerosolpartikeln in der Atmosphäre werden in vielen verschiedenen wissenschaftlichen Gebieten benötigt. Diese reichen vom Gesundheitswesen bis hin zur Klimamodellierung. Deswegen wird im Folgenden eine Ableitungsmethode vorgestellt, die die Einfachstreualbedo und Asymmtrieparameter von Aerosolpartikeln bestimmt. Diese Methode wurde dabei für Messungen im Pearl River Delta, China, in denen oft hohe Luftverschmutzungen auftreten, angewandt. Es werden dazu bodengebundene Messungen der spektralen abwärtsgerichteten Strahlungsflussdichte und Strahldichte, gekoppelt mit Strahlungsübertragungsrechnungen durchgeführt. Um die aerosol-optischen Parameter ableiten zu können, wird als zusätzliche Randbedingung die aerosol-optische Dicke (AOD) benötigt. Sonnenphotometermessungen liefern dabei zum einen die AOD und zum anderen die aerosoloptische Eigenschaften, die mit den Ergebnissen der Ableitungsmethode verglichen werden. Dabei wurden für große AOD-Werte (über 0.5) gute Übereinstimmungen zwischen beiden Methoden festgestellt werden. Für AOD-Werte kleiner als 0.5 und bei bewölkten Bedingungen zeigt die Methode große Unsicherheiten, weil die Parameter zu empfindlich auf diese Begebenheiten reagieren.

1. Introduction

Aerosol particles have an impact on various aspects of the Earth's ecosystem. By scattering or absorption of solar radiation, aerosol particles influence the Earth's radiation budget, but may also alter cloud processes (Boucher et al., 2013). Megacities are a significant source for anthropogenic aerosol particles (Alpert et al., 2012; Cassiani et al., 2013), in particular black carbon particles which show significant uncertainties in the estimation of their radiative forcing (Boucher et al., 2013).
Megacities are cities with a population of over ten million. In the last decades the number of megacities and their inhabitants has increased faster than ever before (Molina and Molina, 2004). Especially health problems for the inhabitants of these major cities can appear during strong smog situations. A major region with heavy smog events are megacities in Asia (Tie and Cao, 2009; Lelieveld et al., 2015).
Aerosol particles show large inhomogeneities in time and space. Therefore, it is important to have algorithms, which derive the aerosol optical properties with high resolution. Ground-based irradiance and radiance measurements were performed, during the "Megacities – Megachallenges" project. Out of it, a new algorithm to derive the aerosol optical properties as asymmetry parameter and single scattering albedo were developed and validated against sun photometer data.

2. Basics

The spectral irradiance describes the flux of radiant energy, which incidents on a flat (horizontal) surface. Every single photon reaching the horizontal surface contributes to the irradiance with a weight that is determined by the cosine of its incident angle. The unit of the spectral irradiance is W m^{-2} nm^{-1}. In contrast to the irradiance, the radiance refers only to a certain solid-angle rather than an entire hemisphere. Consequently the unit of the spectral radiance is W m^{-2} sr^{-1} nm^{-1}. The attenuation of solar radiation by atmospheric constituents is described by the Beer-Lambert-Bouguer law. Fig. 1 shows the schematics for a slant path through the atmosphere.

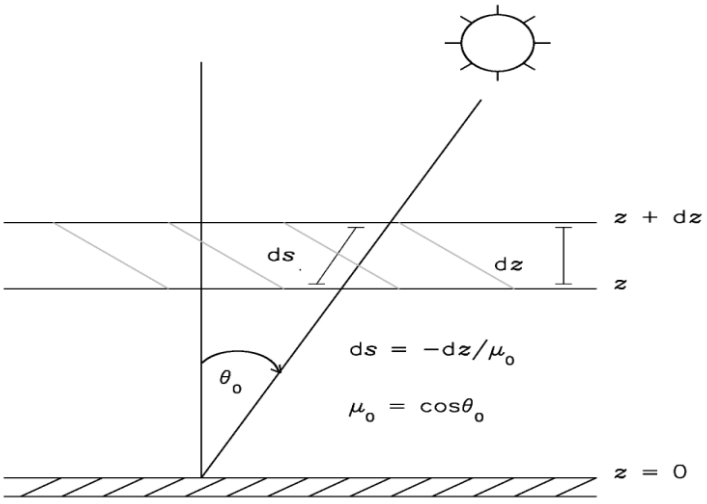

Fig. 1: Description of the geometry in a plane parallel atmosphere after Wendisch and Yang, (2012).

The AOD describes the column integral of the atmospheric extinction of solar radiation by aerosol particles. Θ_0 denotes the solar zenith angle (SZA). The extinction coefficient is composed of the absorption and the scattering coefficient. The single scattering albedo (SSA) is the ratio of scattering to extinction coefficient. That means if the single scattering albedo is equal to 1, then there is only scattering, and if the single scattering albedo is equal to 0, then there is only absorption.
The phase function describes the probability of a scattering event dependent on the scattering angle. The asymmetry parameter (g) can be described as a parametrization of the scattering phase function as an integral about all solid angles. The asymmetry parameter states in which direction the radiation will be mainly scattered. An asymmetry parameter of +1 means only forward scattering and -1 means only backward scattering. If the asymmetry parameter is equal to 0, then the scattering is isotropic, i.e., for every direction the amount of scattered radiation is equal (Wendisch and Yang, 2012). SSA, g and AOD are important quantities to describe the extinction of radiation by aerosol particles (Ruiz-Arias et al., 2014). Present methods to derive these properties are based on measurements of the direct and diffuse irradiance. The currently most common methods to derive the quantities are satellite observations (Remer et al., 2005, Levy et al., 2007) and sun photometer measurements (Holben et al., 1998). But these methods have restrictions. The sun photometer measurements have a low spatial coverage and the satellite measurements still have large uncertainties, especially over land and urban surfaces. Therefore is it important to investigate new approaches to derive aerosol optical properties.

3. Project "Megacities – Megachallenges"

The "Megacities – Megachallenges" project was initiated to answer upcoming questions due to the dynamic expansion of megacities. The project included several different disciplines to cover all important aspects of the development of megacities (as Dhaka in Bangladesh, and Guangzhou in the Pearl River Delta in China).
The data, as described below, were measured in Guangzhou, the capital city of the province Guangdong in the Pearl River Delta. More than eleven million people are living within the megacity Guangzhou.
Ground-based measurements were performed in Guangzhou from November 3, 2011 until January 2, 2012 on the roof of a hotel, unaffected from shadowing by vegetation or buildings. The main instrument for this study, the Compact Radiation Measurement System (CORAS) was deployed together with a sun photometer (Holben et al., 1998), a LIDAR (Althausen et al., 2009) and the imaging spectroradiometer AisaEagle (Schäfer et al., 2013).

4. Instrumentation

CORAS measures spectral downward irradiance and radiance covering a wavelength range between 350 and 2000 nm (Brückner et al., 2014). Each optical inlet is

connected to a system of two grating photodiode array spectrometers via optical fibers. While the irradiance optical inlet measures radiation from the entire upper hemisphere, the upward looking radiance inlet has a field of view of 2°.
CORAS was calibrated with a 1000 W standard calibration lamp and a hemispheric sphere traceable to NIST (National Institute of Standards and Technology). Different corrections are necessary in order to derive calibrated radiation data in physical units from the raw signal. The steps are a dark current correction, the pixel-wavelengths assignment (based on spectral calibration), a transfer calibration in order to account for radiometric differences between laboratory and field, and a cosine correction of the irradiance optical inlet.
The different corrections result in a total measurement uncertainty of 5 % for the irradiance and 10 % for the radiance. Detailed descriptions of the measurement system are provided by Mey (2012) and Brückner et al. (2014). To verify the CORAS measurements, radiative transfer simulations using the "library of radiative transfer routines and programs" (libRadtran) (Mayer and Kylling, 2005) were performed. A cloud free situation was chosen to minimize the uncertainty of the input variables. The vertical extinction profile of the aerosol particles was determined by concurrent LIDAR measurements. The sun photometer delivered the aerosol optical properties as the AOD, the single scattering albedo and the asymmetry parameter for the simulation. Profiles of temperature, pressure, and gases like water vapour, ozone, nitrous oxide, carbon monoxide and methane were taken from Anderson et al. (1986). Further input variables were the extraterrestrial solar spectrum from Gueymard (2003) and the solar zenith and azimuth angles. The used radiative transfer solver was disort2 (Nakajima and Tanaka, 1988; Stammes et al., 2000). The simulated spectral range was from 300 to 1100 nm, and the simulated quantities were the spectral radiance and irradiance.

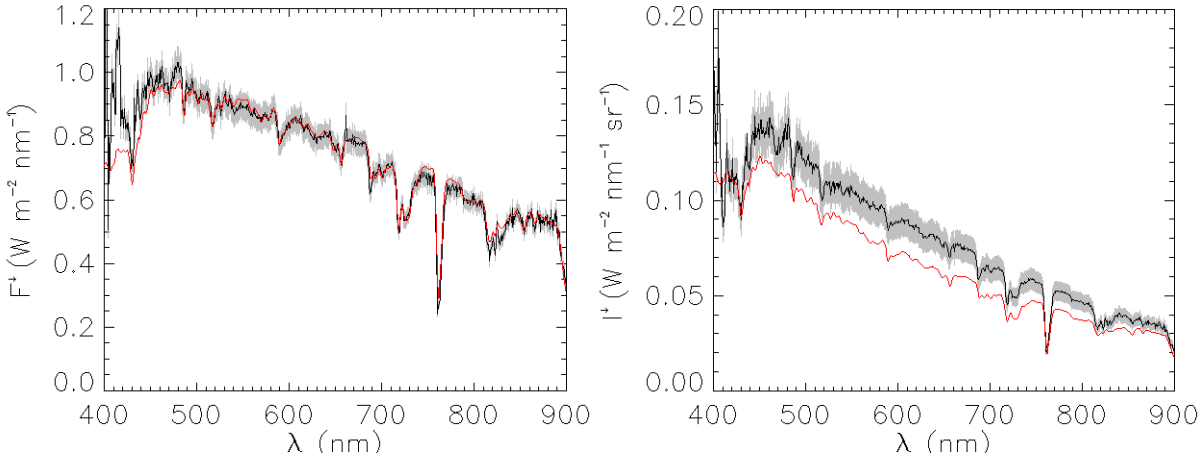

Fig. 2: Comparison between simulation (red) and measurement (black) of the downward irradiance (left) and radiance (right).

Fig. 2 shows measured and simulated irradiance and radiance spectra for clear sky condition on the December 31, 2011, 11:23 local time with a zenith angle of 53°. Local time is UTC+8 hours. The irradiance shows a good agreement between the simulation (red) and the measurement (black) within the measurement uncertainty. The mean deviation is below 3 %. The deviation between the simulated and measured radiance is larger with 15 % with a systematic bias, probably because of high

sensitivity to the model input parameter. Therefore the radiance values are additionally compared to measurements of AisaEagle.
Fig. 3 shows a comparison between CORAS (black) and AisaEagle (red) data. The opening angle of the AisaEagle of 36° distributed over 1024 spatial pixels is much larger than the opening angle of CORAS (2°). For the comparability only the center spatial pixel of the AisaEagle pointing in zenith direction was chosen. The AisaEagle spectra are within the error bars of CORAS (grey) indicating good agreement between both instruments. The mean derivation for the whole case is about 5 %. The derivation for the shown example is 3 %. This shows that also the radiance values are sufficiently accurate to use them for the derivation algorithm.

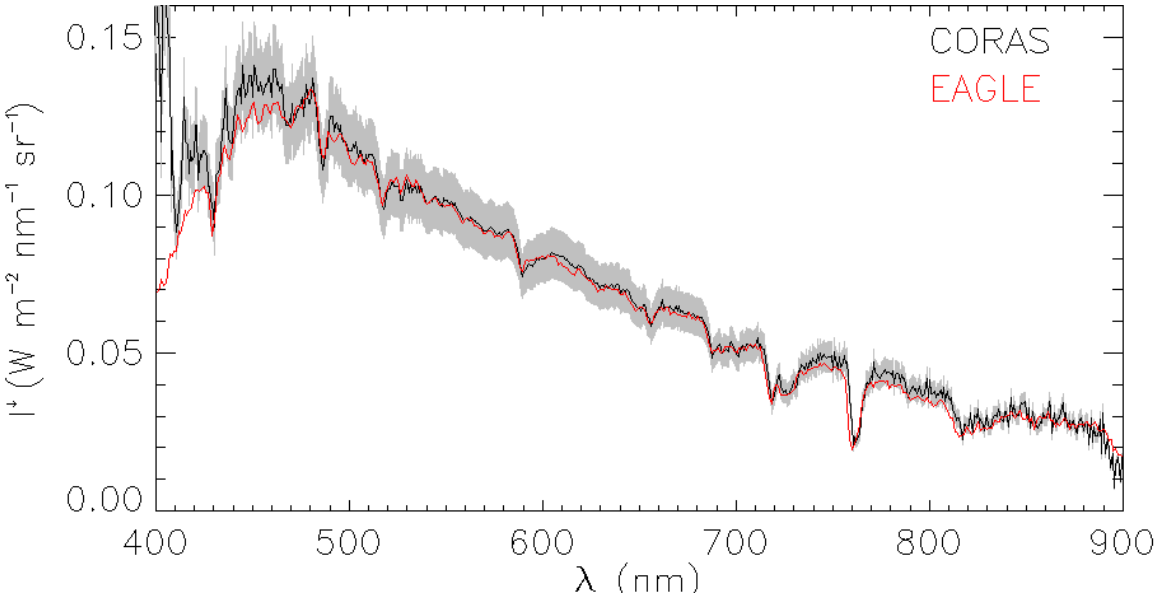

Fig. 3: Comparison between AisaEagle (red) and CORAS (black) of the downward radiance from November 15, 2011 at 5:03 UTC.

5. Derivation of aerosol optical properties

The extinction of solar radiation by aerosol particles depends on the amount of aerosol particles and their scattering/absorption properties. With knowledge of the AOD the directional dependence of the extinction (in terms of the asymmetry parameter) and the fraction of scattering on the total extinction (single scattering albedo) can be estimated from concurrent irradiance and radiance data which are highly sensitive to these parameters.
Radiative transfer calculations using libRadtran were performed for a set of single scattering albedos and asymmetry parameters to create lookup tables (LUTs). In general the optical parameters are spectral dependent. Here only results for the 500 nm wavelengths are shown. The single scattering albedo was varied from 0.8 to 1.0 and the asymmetry parameter from 0.6 to 0.9 in steps of 0.02. Each grid was interpolated, because of the fact that small changes result in larger uncertainties. The steps of the aerosol optical properties were interpolated to 0.005. The model input was additionally adapted to the solar zenith and solar azimuth angle (SZA, SAA) for each time step of the selected radiation measurement. Finally, the lookup tables were searched for the

best match of the radiance and irradiance pairs. For better illustration the LUTs were plotted as grids as shown in Figure 4.
The grid is calculated for a certain SZA and AOD, for a variable set of asymmetry parameter (*g*) and single scattering albedo values (SSA). If the SSA raises both radiation quantities also become larger. That is because larger SSA values mean less absorption. For variations in *g* the properties of the radiation values is not as clear as for SSA. Larger values of *g* lead to larger values of the irradiance but smaller values of the radiance. That is because larger values of *g* leads to less scattering in the sideward direction and less scattering in the 2° opening angle of the sensor. The irradiance values become larger because of less scattering in the backward direction. Additionally, a radiance/irradiance measurement pair and its uncertainty range (red bars) are plotted. Each pair of SSA and *g* within this range is a possible solution. Instead of taking the mean over all values within this area, the median is calculated as the most likely solution. As can be seen in Fig. 5, the histograms of both parameters do not follow a symmetric distribution but a shift of the maximum to the right. The reason for this is that there is no equidistant distance between the isolines of constant SSA and *g*. As a measure of the width of the distribution the standard deviation is given.

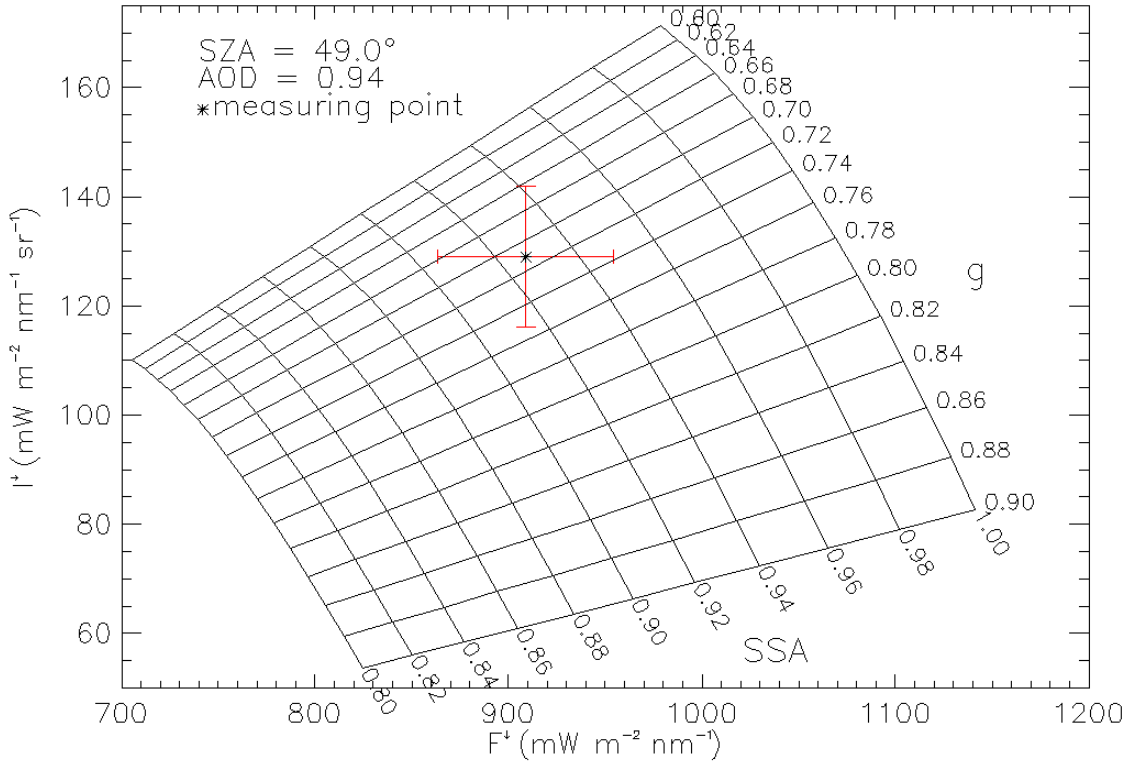

Fig. 4: Simulated grid of down welling radiance vs. irradiance as function of single scattering albedo (SSA) and asymmetry parameter (g) with a measurement point (black star) and the corresponding range of uncertainty (red bars) for a fixed point of time.

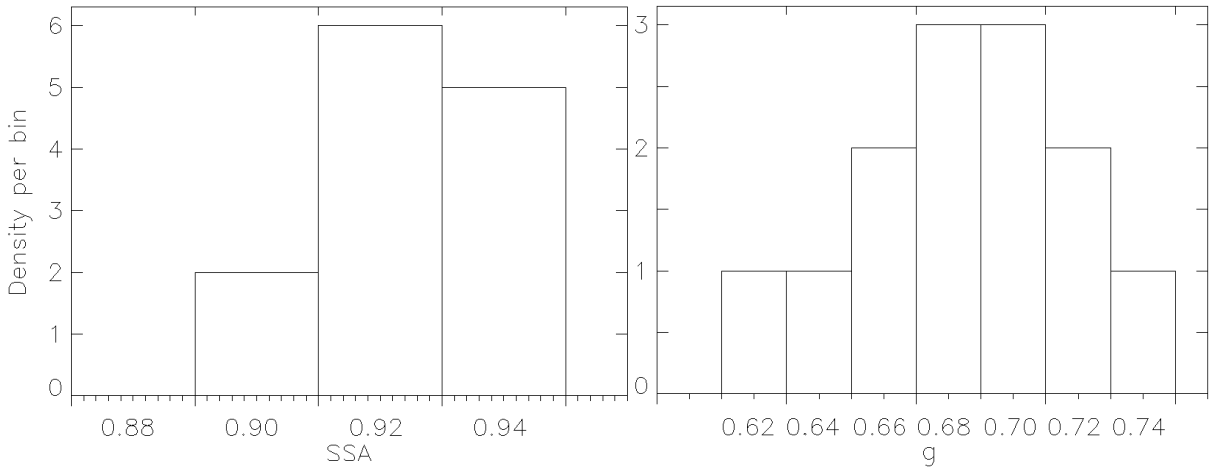

Fig. 5: Example histograms of the aerosol optical properties (a) SSA and (b) g which are lying within the range of uncertainty.

6. Measurement examples

Different measurement cases were analyzed by using the algorithm presented in Section 5. The aerosol optical properties derived with the algorithm were compared with the concurrent sun photometer measurements. All radiation data were filtered with respect to atmospheric conditions and availability of supplement datasets as from the sun photometer and the LIDAR. A broad spectrum of different conditions was found with AODs between 0.1 and 1.1. The single cases cover time intervals from 30 minutes up to more than two hours. For better comparison the AOD had to be as constant as possible within this time intervals. The measurements of the sun photometer were quite irregular. Hence, the mean over the period was used. The resolution for the single CORAS measurements are 20s and for the LIDAR 30s. Cloud cases were excluded with the help of the sun photometer and LIDAR data. Two examples of the analyzed cases are shown in the following.

6.1 Example with high AOD

The first case is dated from November 29, 2011 for a period between 0:47 and 1:30 UTC. The measured AOD was 1.14±0.025, the largest aerosol optical depth of all analyzed cases. The sun photometer value for the single scattering albedo amounted to 0.922±0.028 and the value of the asymmetry parameter was 0.74±0.022. The solar zenith angle ranged between 67° at the beginning and 59° at the end of the period.

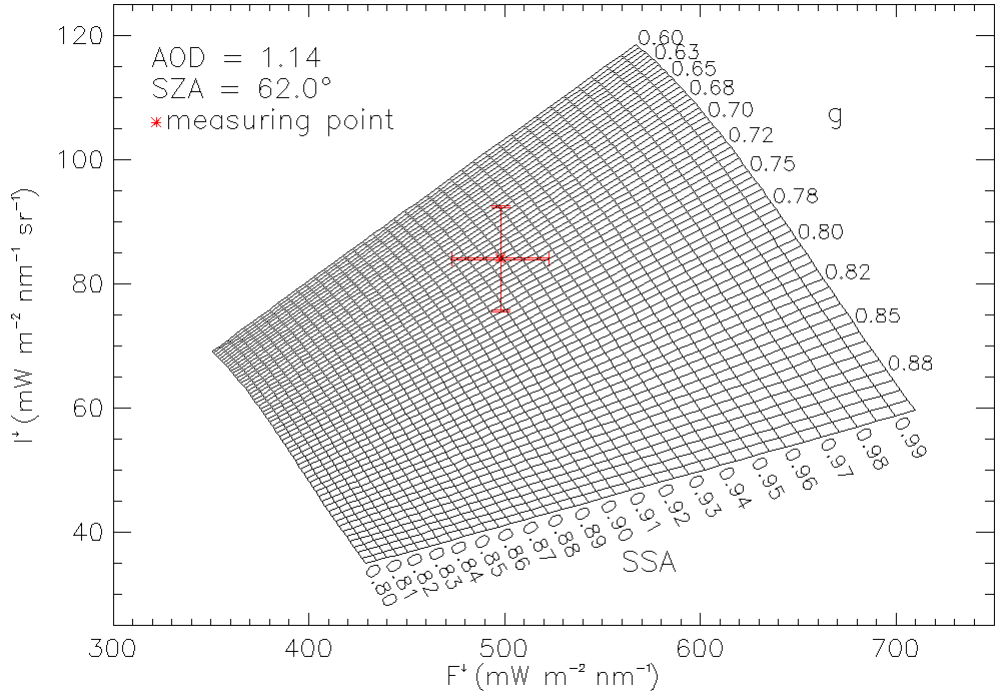

Fig. 6: A LUT grid for the derivation of the aerosol optical properties with two measurement points (red) from November 29, 2011 at 1:16 UTC, similar to Fig. 4.

Fig. 6 shows, that the measurements fall into the grid with realistic values of *g* and SSA. The derived single scattering albedo was 0.92±0.01 and the derived asymmetry parameter was 0.72±0.029. For this particular case all data points sampled within the time period were falling in the LUT grid and show good agreement with concurrent sun photometer data within the range of uncertainty. Also other studies (Alam et al., 2011) have shown similar results for typical SSA-values (0.92) in megacities in winter months.

This proves that the algorithm is operating well for this case. Fig. 7 shows the time series of *g* and SSA with a temporal resolution of 20 s, as a function of time and SZA. The derived values of the single scattering albedo are plotted as plus signs and the asymmetry parameter values as stars. Furthermore, the uncertainty of the derived parameters is given as a grey area around the measurement points which is larger for the asymmetry parameter than for the single scattering albedo due to larger measurement uncertainty of the radiances (10 %) compared to that of the irradiance (5%).

The single scattering albedo is quite constant over the entire period. The small fluctuations are indicators for inhomogeneities within the atmosphere, either by aerosol particles or subvisible clouds. The asymmetry parameter shows a larger variation over the same time. A possible reason might be that small changes of the radiance values have a larger influence on the derived asymmetry parameter than on the SSA, because the radiance is a strongly directional dependent measure of radiation. However, the algorithm works quite well in this case and all derived values are within a realistic range and are quite near to the values of the sun photometer measurements.

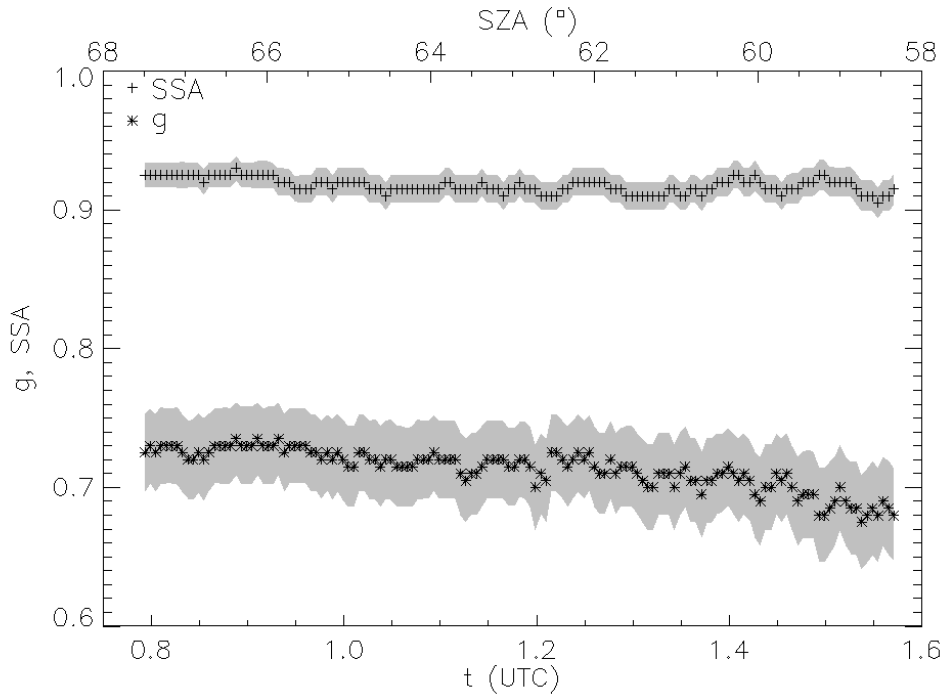

Fig. 7: Time series of the aerosol optical properties g and SSA with their retrieval uncertainties from November 29, 2011.

6.2 Example with low AOD

The second case illustrates the limitation of the method for low AODs. Data from December 11, 2011 between 5:56 and 8:36 UTC were evaluated. The SZA varied from 51° to 76° in this period. Sun photometer measurements resulted in a mean AOD of 0.251±0.005, a mean single scattering albedo of 0.866±0.007 and a mean asymmetry parameter of 0.668±0.008.

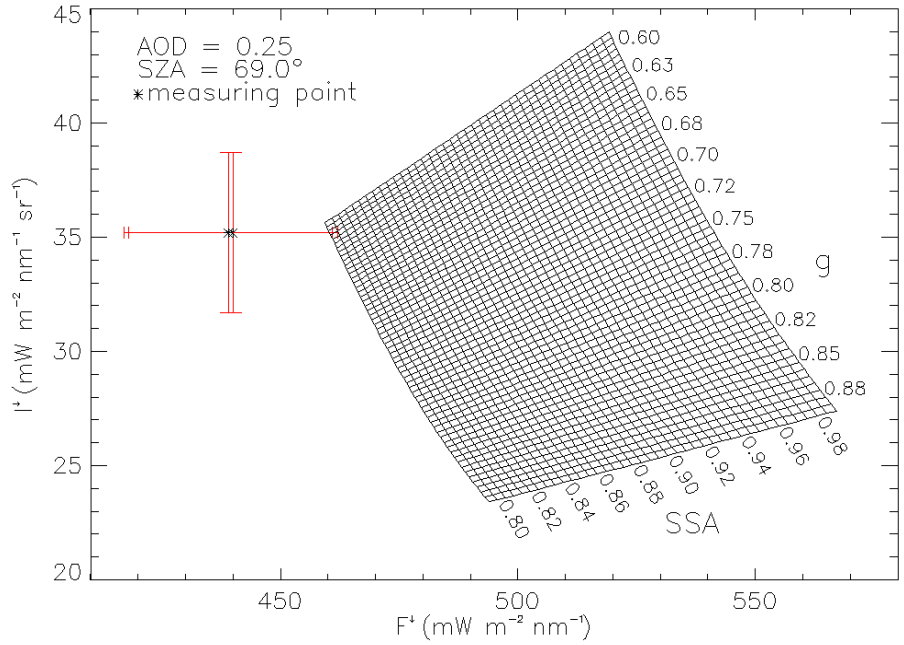

Fig. 8: A LUT grid for the derivation of the aerosol optical properties with two measurement points (red) from December 11, 2011 at 7:51 UTC.

Fig. 8 presents the corresponding LUT-grid for measurements at 7:51 UTC. Obviously the radiance/irradiance pairs are not within the grid. This issue occurred for the entire period increasing the number of *g* and SSA parameters to lower values to match the measured data would lead to unrealistic retrieval results. The algorithm does not work for this example. Similar results have been found for all cases with low AOD values. Possible reasons will be discussed in Section 7.

7. Error discussion

The used algorithm underlies several restrictions and is prone to errors. It is necessary to proceed cautiously to reduce the retrieval uncertainty. One restriction to derive the aerosol optical properties by the method is the selection of cloudless conditions. The radiative transfer simulations, which were used to calculate the LUTs, were only performed for cloudless conditions. The angular distribution of the radiance is highly sensitive to the presence of clouds which directly has an effect on the derived asymmetry parameter.

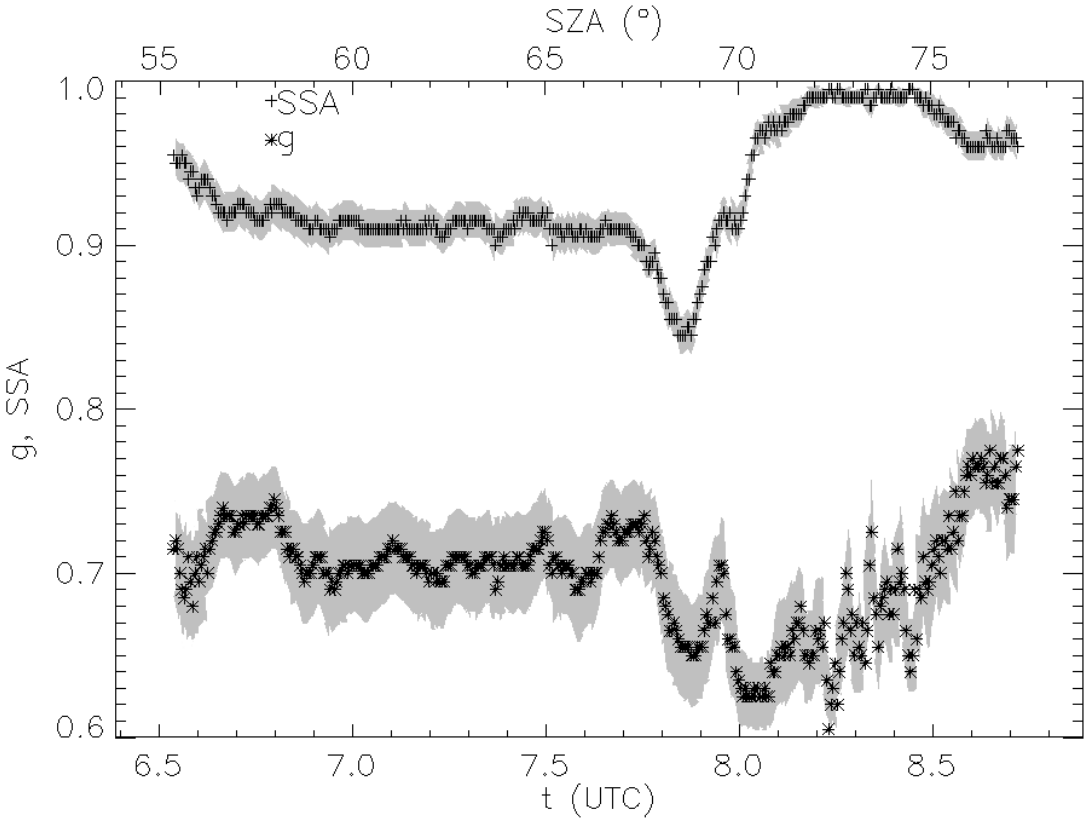

Fig. 9: Time series of the aerosol optical properties with their estimated uncertainty from January 1, 2012.

Fig. 9 shows a time series of the aerosol optical properties with an approaching cloud. Quite constant values of the aerosol optical properties could be derived in the first half of the time series during clear sky conditions. After the cloud is approaching *g* and SSA is first decreasing and increasing afterwards, probably related to the directional distribution of the clouds.

Besides the careful selection of cloudless cases also other constraints have to be considered to gain reliable retrieval results. In general, the relation of irradiance and radiance must not be too sensitive to changes of the aerosol properties, because the measurement uncertainties of both radiative quantities can result in large deviations of the retrieved *g* and SSA. Mainly two parameters determine the sensitivity of the irradiance – radiance relation on the aerosol properties, namely, the SZA and the AOD. Fig. 10 shows the variation of the LUT-grids for different SZAs for the same scaling of the abscissa and ordinate. The difference in the size of the two LUT-grids is distinctive. The higher the SZA the less radiation reaches the optical inlets, and small uncertainties in the radiance and the irradiance lead to broad distributions of the estimated *g* or SSA values. Since the SZA has a considerably effect on the LUT-grid, the horizontal alignment of the optical inlets has to be as accurate as possible. The comparison of the measurements with radiative transfer simulations as presented in Section 3 did not show any evidence for a misalignment of the optical inlets. An offset angle in direction towards the sun would lead to an enhancement of radiation or to a decrease of radiation in case the sensor is misaligned away from the sun.

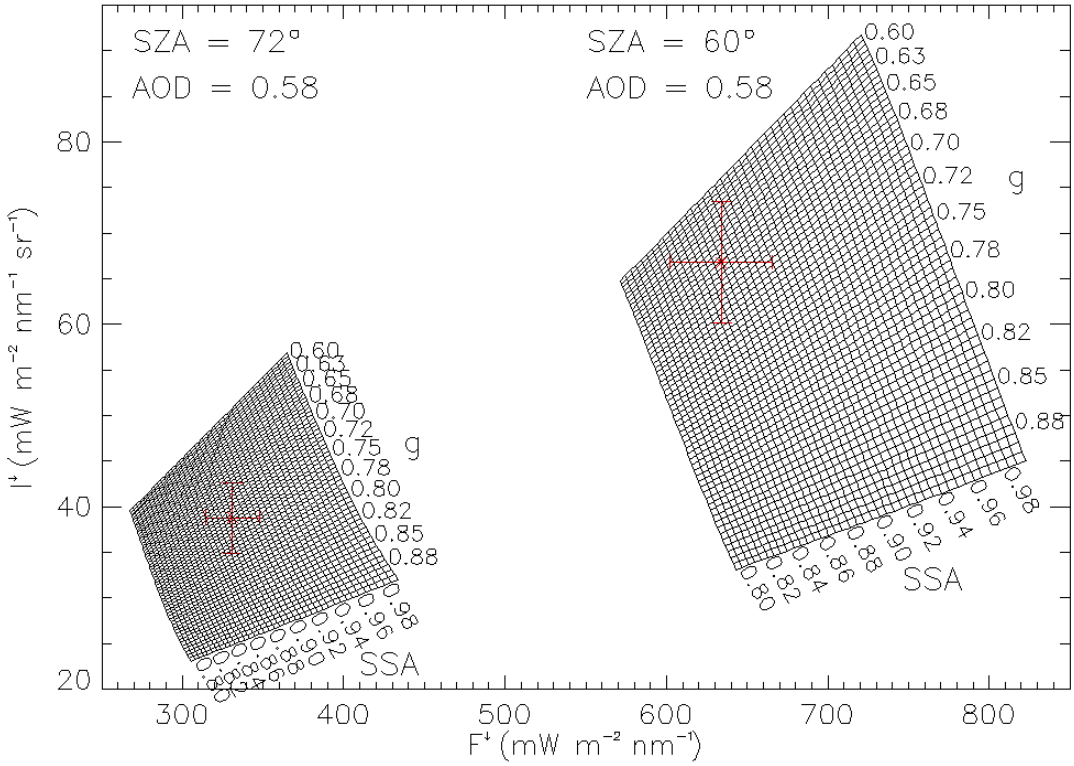

Fig. 10: Two different LUT-grids for the derivation of the aerosol optical properties with measurement points (red) from November 28, 2011. The left grid is from 0:20 UTC (SZA = 72°) and the right one from 1:27 UTC (SZA = 60°).

The second crucial parameter for the retrieval method is the AOD, which is delivered by a sun photometer. The measurement uncertainty of 5 % also leads to an additional source of the retrieval uncertainty, in particular for low AODs as shown in one of the measurement examples above.
Fig. 11 shows the influence of the AOD on the LUT-grid for three AOD-values ranging between 0.1 and 1.0. The three LUT-grids were calculated with the same conditions for all three cases, except a variation of the AOD. It is also noticeable that

the absolute values of the irradiance are largest for lower AODs, while the radiances are largest for high AODs. The reason for this is simple; if there are fewer particles then less radiation is scattered in the direction of the opening angle of the radiance's optical inlet. On the other hand a lower AOD results in less extinction and consequently in larger values of the irradiance.
The larger the AOD, the larger becomes the distance between the values in the LUTs as visualized in the LUT-grids. For large AODs the LUT-grids are more stretched than for lower AODs. Consequently, the influence of the measurement uncertainties on the retrieval accuracy gets lower since the spacing between the grid points increases. But for small AODs the measurements have to be much more precise than given. Therefore, it is not possible to derive realistic aerosol optical properties with the help of the algorithm for AODs smaller than about 0.5.

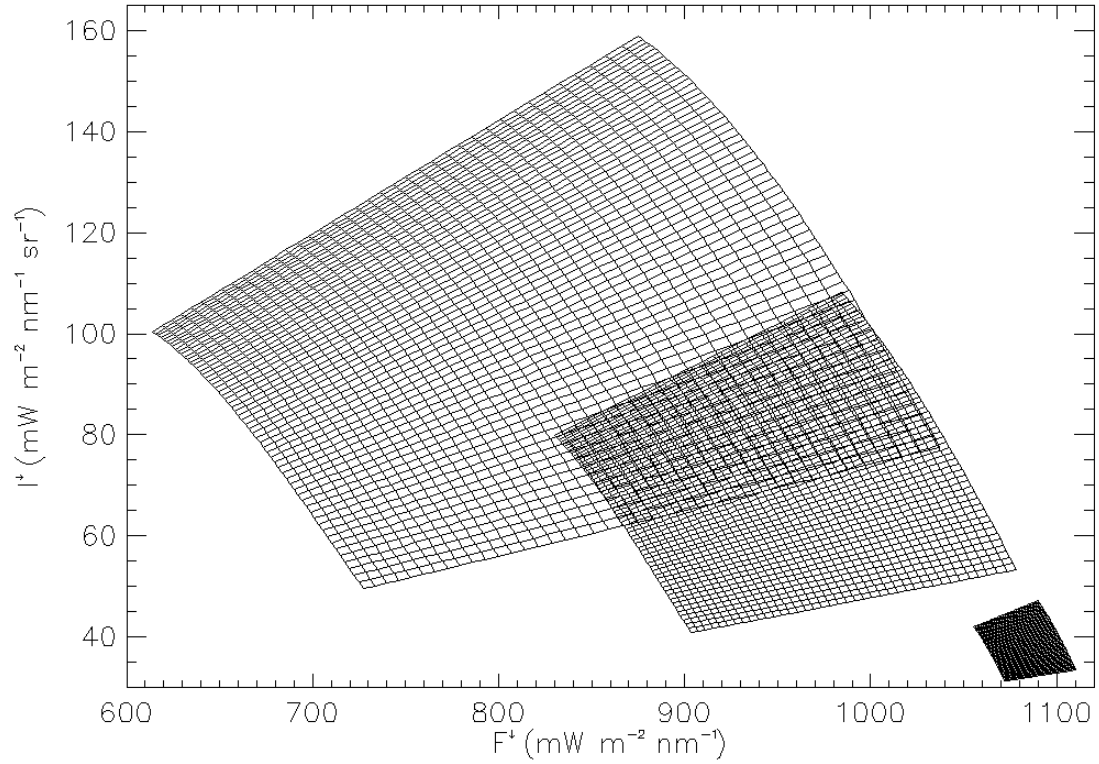

Fig. 11: Three grids for the derivation of the aerosol optical properties at different AODs: large LUT-grid, AOD=1.0; medium LUT-grid, AOD=0.5; small LUT-grid, AOD=0.1.

8. Summary and outlook

The present study has used a new approach to derive aerosol optical properties (asymmetry parameter and single scattering albedo) with ground-based radiation measurements. Concurrent observations of the downward radiance and irradiance were used to test the new approach for data gained during the "Megacities – Megachallenges" project in the Pearl River Delta, China. First of all, the CORAS measurements were compared to radiative transfer simulations for clear sky conditions to validate the data quality. For this comparison the model input of the aerosol properties was taken from LIDAR and sun photometer measurements. It was shown

that irradiance data could be reproduced by the simulation. The radiance data was additionally compared to AisaEagle measurements. A high consistency between the two data sets could be shown.
In a next step LUTs were created out of given AODs from the sun photometer and SZAs for a set of aerosol properties. These LUTs were applied to selected clear sky cases. It has been shown that the relation of both radiative quantities significantly depends on the aerosol properties, but its sensitivity is highly variable with AOD and SZA. On the one hand the retrieval uncertainty is influenced by the measurement uncertainty of the irradiance, radiance, and the AOD but also on the sensitivity of the parameters.
Examples with high and low AODs were presented showing that only for high AODs (larger than 0.5) the aerosol optical properties could be derived in a comparable range to the sun photometer measurements of *g* and SSA.
In order to improve the algorithm, it is necessary to raise the accuracy of the measurements. Especially the AODs have to be measured with a higher temporal resolution. Furthermore, it is recommended to use an all-sky-camera to identify clear sky cases better. The LUTs have to be calculated for individual conditions adapted more precisely with respect to extinction by gases and molecules. More measurements are necessary to get a more test the applicability of the method. In general the method can be applied for cases where only AODs are available instead of full information of the aerosol properties (e.g., satellite or sun photometer measurements).
In conclusion, the algorithm provides good results for large AODs now, but further investigations are necessary for cases of small AODs to estimate the restrictions of the method more systematically.

9. References

Alam, K., Trautmann, T., and Blaschke, T., 2011: Aerosol optical properties and radiative forcing over mega-city Karachi, Atmos. Res., 101, 773–782, doi: 10.1016/j.atmosres.2011.05.007.

Althausen, D., Engelmann, R., Baars, H., Heese, B., Ansmann, A., Müller, D., and Komppula, M., 2009: Portable Raman Lidar Polly^{XT} for Automated Profiling on Aerosol Backscatter, Extinction, and Depolarization, J. Atmos. Oceanic Technol., 26, 2366–2378, doi: http://dx.doi.org/10.1175/2009JTECHA1304.1.

Alpert, H. R., Connolly, G. N., Biener, L., 2012: A prospective cohort study challenging the effectiveness of population-based medical intervention for smoking cessation, Tob. Control, 22, Issue 1, 32-37, doi: 10.1136/tobaccocontrol-2011-050129.

Anderson, G. P., Clough, S. A., Kneizys, F. X., Chetwynd, J. H., Shettle, E. P., 1986: AFGL Atmospheric Constituent Profiles (0-120km), Optical Physic Division, Air Force Geophysics Laboratory, Hanscom AFB, MA 01731, Environ. Res. Paper, No. 954.

Boucher, O., Randall, D., Artaxo, P., Bretherton, C., Feingold, G., Forster, P., Kerminen, V.-M., Kondo, Y., Liao, H., Lohmann, U., Rasch, P., Satheesh, S. K., Sherwood, S., Stevens, B., and Zhang, X. Y., 2013: Clouds and Aerosols. In: Climate Change 2013: The Physical Science Basis. Contribution of Working Group I to the Fifth Assessment Report of the Intergovernmental Panel on Climate Change [Stocker, T.F., D. Qin, G.-K. Plattner, M. Tignor, S.K. Allen, J. Boschung, A. Nauels, Y. Xia, V. Bex and P.M. Midgley (eds.)]. Cambridge University Press, Cambridge, United Kingdom and New York, NY, USA.

Brückner, M., Pospichal, B., Macke, A., and Wendisch, M., 2014: A new multispectral cloud retrieval method for ship-based solar transmissivity measurements, J. Geophys. Res. Atmos., 119, Issue 19, Pages 11, 338–11,354, doi: 10.1002/2014JD021775.

Cassiani, M., Stohl, A., and Eckhardt, S., 2013: The dispersion characteristics of air pollution from the world's megacities, Atmos. Chem. Phys., 13, 9975–9996, doi: 10.5194/acp-13-9975-2013.

Gueymard, C., 2003: The sun's total and spectral irradiance for solar energy applications and solar radiation models, Solar Energy, 76, 4, 423-453, doi: 10.1016/j.solener.2003.08.039.

Holben, B. N., Eck, T. F., Slutsker, I., Tanré, D., Buis, J. P., Setzer, A., Vermote, E., Reagan, J. A., Kaufman, Y. J., Nakajima, T., Lavenu, F., Jankowiak I., and Smirnov, A., 1998: AERONET - A Federated Instrument Network and Data Archive for Aerosol Characterization, Remote Sens. Environ., 66, 1-16, doi: 10.1016/S0034-4257(98)00031-5.

Lelieveld, J., Evans, J. S., Fnais, M., Giannadaki, D., and Pozzer, A., 2015: The contribution of outdoor air pollution sources to premature mortality on a global scale, Nature, 525, 367–371, doi: 10.1038/nature15371.

Levy, R. C., Remer, L. A., Mattoo, S., Vermote, E. F., and Kaufman, Y. J., 2007: Second-generation operational algorithm: Retrieval of aerosol properties over land from inversion of Moderate Resolution Imaging Spectroradiometer spectral reflectance, J. Geophys. Res., 112, D13211, doi: 10.1029/2006JD007811.

Mayer, B., and Kylling, A., 2005: Technical note: The libRadtran software package for radiative transfer calculations – description and examples of use, Atmos. Chem. Phys., 5, 1855–1877, doi: 10.5194/acp-5-1855-2005.

Mey, B. S., 2012: Einfluss der Bodenalbedo und Bodenreflektivität von urbanen Oberflächen auf die Ableitung der optischen Dicke von Aerosolpartikeln aus Satellitenmessungen, Dissertation, Qucosa, 135, nbn-resolving.de/urn:nbn:de:bsz:15-qucosa-113056.

Molina, M. J., and Molina, L. T., 2004: Megacities and Atmospheric Pollution, J. Air & Waste Manage. Assoc., 54, 644–680.

Nakajima, T., and Tanaka, M., 1988: Algorithms for radiative intensity calculations in moderately thick atmospheres using a truncation approximation, J. Quant. Spectrosc. Radiat. Transf., 40 (1), 51–69, doi: 10.1016/0022-4073(88)90031-3.

Remer, L. A., Kaufman, Y., Tanré, D., Mattoo, S., Chu, D., Martins, J., Li, R.-R., Ichoku, C., Levy, R., Kleidman, R., Eck, T., Vermote, E., and Holben, B., 2005: The MODIS aerosol algorithm, products, and validation, J. Atmos. Sci., 62, 947–973, doi: http://dx.doi.org/10.1175/JAS3385.1.

Ruiz-Arias, J. A., Dudhia, J., and Gueymard, C. A., 2014: A simple parameterization of the short-wave aerosol optical properties for surface direct and diffuse irradiances assessment in a numerical weather model, Geosci. Model Dev., 7, 1159–1174, doi: 10.5194/gmd-7-1159-2014.

Schäfer, M., Bierwirth, E., Ehrlich, A., Heyner, F., and Wendisch, M., 2013: Retrieval of cirrus optical thickness and assessment of ice crystal shape from ground-based imaging spectrometry, Atmos. Meas. Tech., 6, 1855–1868, doi: 10.5194/amt-6-1855-2013.

Stamnes, K., Tsay, S.-C., Wiscombe, W. J., and Laszlo, I., 2000: DISORT, a general-purpose fortran program for discrete-ordinate-method radiative transfer in scattering and emitting layered media: documentation of methodology. DISORT Report, version 1.1.

Tie, X., and Cao, J., 2009: Aerosol pollution in China: Present and future impact on environment, Particuology, 7, 426–431, doi: 10.1016/j.partic.2009.09.003.

Wendisch, M., and Yang, P., 2012: Theory of Atmospheric Radiative Transfer, Wiley-VCH Verlag GmbH & Co. KGaA, Weinheim, Deutschland, ISBN: 978-3-527-40836-8, p. 70-72, p. 146-174.